Hindawi
Canadian Respiratory Journal
Volume 2020, Article ID 1237418, 16 pages
https://doi.org/10.1155/2020/1237418

Review Article

Contribution of CT Features in the Diagnosis of COVID-19

Houdong Zuo

Sichuan Key Laboratory of Medical Imaging, Department of Radiology, Affiliated Hospital of North Sichuan Medical College, Nanchong, Sichuan 637000, China

Correspondence should be addressed to Houdong Zuo; zuohoud@163.com

Received 8 July 2020; Revised 19 September 2020; Accepted 28 October 2020; Published 16 November 2020

Academic Editor: Theodoros I. Vassilakopoulos

The outbreak of novel coronavirus disease 2019 (COVID-19) first occurred in Wuhan, Hubei Province, China, and spread across the country and worldwide quickly. It has been defined as a major global health emergency by the World Health Organization (WHO). As this is a novel virus, its diagnosis is crucial to clinical treatment and management. To date, real-time reverse transcription-polymerase chain reaction (RT-PCR) has been recognized as the diagnostic criterion for COVID-19. However, the results of RT-PCR can be complemented by the features obtained in chest computed tomography (CT). In this review, we aim to discuss the diagnosis and main CT features of patients with COVID-19 based on the results of the published literature, in order to enhance the understanding of COVID-19 and provide more detailed information regarding treatment.

1. Introduction

Coronavirus disease 2019 (COVID-19) is a highly contagious viral disease that first appeared in Wuhan, Hubei Province, China, at the end of December 2019 and rapidly spread across the country and worldwide. In January 2020, the World Health Organization (WHO) announced COVID-19 to be a major global health emergency (https://www.who.int/emergencies/diseases/novel-coronavirus-2019/situation-reports/). As of 5 July 2020, the WHO reported a total of 11,125,245 cases and 528,204 deaths due to COVID-19 (Situation report-167). At present, real-time reverse transcription-polymerase chain reaction (RT-PCR) is considered to be the standard diagnostic approach, but RT-PCR of viral nucleic acids may sometimes provide false-negative results in the initial tests [1, 2]. Therefore, some studies have reported the significance of computed tomography (CT) in diagnosing COVID-19 with higher sensitivity [3, 4]. Additionally, examination with CT has been recommended as a key tool for diagnosing and monitoring disease progression and follow-up by the National Health Commission of China (available at http://www.gov.cn/zhengce/zhengceku/2020-02/19/content_5480948.htm). The combined application of RT-PCR and CT may have advantages over single test alone and may increase the accuracy and sensitivity of diagnosis, although the algorithm of combining RT-PCR and early chest CT has not been fully studied yet and is still to be proven with more further studies [5, 6]. Different CT features have been reported by various studies at different time points, but some typical and primary characteristics can be generalized, including the bilateral and lower distribution of ground-glass opacities (GGOs), crazy-paving patterns, and consolidations in the peripheral lung area [7, 8]. With the increasing number of studies and the rise in the number of cases, more CT signs are being increasingly reported, including traction bronchiectasis, vascular enlargement, and reversed halo sign, among others [9, 10]. In order to have a better understanding of COVID-19 and achieve accurate diagnosis, as well as improve treatment and management, it is highly encouraged to focus on the diversity of COVID-19. In this review, we therefore aimed to discuss the diagnosis of COVID-19 and delineate the typical CT features based on the latest published literature, for facilitating the diagnosis and treatment of COVID-19.

2. The Literature Search

The COVID-19-related literature studies in this review were searched till 30 September 2020. And all the literature studies were searched based on the PubMed database (https://pubmed.ncbi.nlm.nih.gov/) using the keywords of

"coronavirus," "nCoV," "2019-nCoV," SARS-CoV-2, "COVID-19," "PCR," and "CT." We have also included non-peer-reviewed articles from preprint repositories.

3. Diagnosis of COVID-19

Ever since the outbreak of COVID-19, the development of a fast and accurate diagnostic strategy has been of utmost necessity for the clinical treatment and management of the disease. RT-PCR is presently recognized as the gold standard for the diagnosis of COVID-19 [11, 12]. However, the performance of RT-PCR varies greatly, especially with respect to sensitivity [4, 13, 14]. Some new additional techniques with increased sensitivity for the diagnosis of COVID-19 were developed and demonstrated that this assay had satisfactory reproducibility in terms of cycle threshold [12, 15]. Although the sensitivity of RT-PCR has been improved greatly, the diagnostic assay still shows some false-negative results, which delays the timely treatment of patients [16]. The low or discrepant sensitivity of RT-PCR may be attributed to various reasons that are described hereafter.

First, the absence of a robust reference standard may affect the sensitivity of RT-PCR. When the combination of contact history and CT findings serve as the reference standard and is used in the COVID-19 diagnosis and results in false positives, RT-PCR sensitivity is underestimated, which means the patients without COVID-19 are diagnosed as COVID-19. On the other hand, if the RT-PCR is included in the reference standard, it may lead to "incorporation bias," which results in overestimation of RT-PCR sensitivity in turn. The use of repeated RT-PCR testing is likely to underestimate the true rate of false negatives because not all patients in the included studies received repeated testing and those who clinically diagnosed COVID-19 were not considered to have COVID-19 actually [14, 17]. Therefore, RT-PCR with a negative result cannot exclude the possibility of COVID-19 infection and RT-PCR should not be the only criterion for diagnosis, treatment, or patient management decisions. The combination of RT-PCR and clinical features along with medical imaging evaluation facilitates the management of COVID-19 [18, 19]. Second, the sampling site and quality also affect sensitivity. In a study by Wang and coworkers [20], the sensitivity rate of RT-PCR reached 93% highest with the samples from bronchoalveolar lavage fluid (BALF), which was significantly higher than the sputum (72%), nasal swabs (63%), and fibrobronchoscope brush (46%) in COVID-19 patients. Thus, the BALF and sputum were strongly recommended for the COVID-19 diagnosis and detection of viral RNAs [19]. Third, the stage of the COVID-19, which can be interpreted as the viral load consequently, can also affect RT-PCR sensitivity. According to the natural history of the COVID-19 and viral load kinetics in different patients, sampling procedures largely contribute to the false-negative results. Optimum timing for peak viral load during infections caused by COVID-19 has great influence on the sensitivity of RT-PCR, and higher viral load may associate with higher sensitivity [17, 19]. Fourth, the results from RT-PCR using primers in different genes can be affected by viral RNA sequence variation due to the genetic diversity and rapid evolution of this novel coronavirus. False-negative results may occur by mutations in the primer and probe target regions in the novel coronavirus genome [21, 22]. The mismatches between the primers and probes and the target sequences caused by variability can result in decrease in assay performance and potential false-negative results. Finally, technical aspects of sampling may also affect the RT-PCR sensitivity, such as swab materials (should be dacron and not cotton) [23], transportation conditions, and handling of the specimens (different equipment).

Several researchers have proposed that CT scans can serve as an alternative to RT-PCR owing to better sensitivity than RT-PCR [1, 3]. Numerous studies have reported that the rate of detecting positives and the sensitivity of CT are higher than those of RT-PCR, but the observations of different studies vary owing to the differences in the inclusion criteria, reference standard, and the testing time. Consequently, studies that employ different methods produce different outcomes. The sensitivity of chest CT may be lower in confirmed cases of COVID-19 when there are fewer limitations in methodological application. Bernheim and coworkers [10] performed a retrospective study in which more than half of the CT scans were performed within 2 days after the onset of the initial symptoms. The results were proved to be normal, and only one patient with COVID-19 showed negative results in the initial RT-PCR test. This finding indicated that up to 50% of CT scans performed within 2 days of the appearance of initial symptoms were likely to be interpreted as those of a normal, uninfected individual, by an expert panel [24].

Additionally, very little information is available on the specificity of chest CT for COVID-19 owing to its limitations in distinguishing the abnormal CT findings caused by other infections [4], with those caused by COVID-19, although Bai and coworkers reported that this method has high specificity [25]. The best strategy for the diagnosis of COVID-19 appears to be the combination of CT and RT-PCR, which may render the best diagnostic efficacy [2]. He and his coworkers reported a comprehensive strategy where the initial results of RT-PCR were combined with CT. Using this strategy, an increasing number of patients with COVID-19 were correctly diagnosed, and the sensitivity of this strategy was as high as 94% (95% CI: 86–100%). The specificity and accuracy were 100% and 98%, respectively [2] (Table 1).

The discussion regarding the use of RT-PCR and CT will continue. The RT-PCR is recognized as the golden standard in the COVID-19 diagnosis, but there are false negative sometimes. CT has a relative higher sensitivity, whereas the specificity cannot be guaranteed. However, the timely application of CT in patients with COVID-19 is of utmost importance, especially in cases where the initial results of RT-PCR are negative, or in cases with no obvious symptoms but with close contact history. In addition, CT and its findings can also facilitate the stage of COVID-19 and monitor the change and evolution of this disease, which is more crucial to the option of the treatment and the management for the clinicians.

Table 1: The positive rate/sensitivity and specificity of initial RT-PCR and initial CT based on the published studies.

	Biological sample	Reference standard	Initial RT-PCR PT/Sen	Initial RT-PCR Spe	Initial CT PT/Sen	Initial CT Spe
Li et al. [14]	Pharyngeal swab	PCR(+) and CT(+)	37% (226/610)/—	—	—	—
Fang et al. [3]	Throat swab or sputum samples	PCR(+) and CT	—/71% (36/51)	—	—/98% (50/51)	—
Mardani et al. [26]	Pharyngeal swab	PCR(+)	35% (70/200)/—	—	—	—
He et al. [2]	Nasopharyngeal swab, oropharyngeal swab, endotracheal aspirate, or bronchoalveolar lavage	PCR(+) and CT(+)	—/79% (27/34)	100%((95%CI: 100%))	—/77% (26/34)	96% (95% CI: 90–100%)
Wang et al. [6]	Throat swab samples	PCR(+)	—/65% (580/888)	83% (105/126)	—/97% (580/601)	25% (105/413)
Liu et al. [13]	Nasal and pharyngeal swabs, bronchoalveolar lavage fluid, and sputum samples	PCR(+)	38% (1854/4880)/—	—	—	—
Long et al. [1]	Pharyngeal oral and nasal sampling	PCR(+)	—/83.3% (30/36)	—	—/97.2% (35/36)	—
Ai et al. [4]	Throat swab samples	PCR(+)	59% (601/1014)/—	—	88% (888/1014)/97% (580/601)	—
Guan et al. [27]	Nasal and pharyngeal swab specimens	PCR(+)	—	—	82.1% (720/877)/—	—
Bernheim et al. [10]	Bronchoalveolar lavage, endotracheal aspirate, nasopharyngeal swab, or oropharyngeal swab	PCR(+)	88% (90/102)/—	—	78% (94/121)/—	—
Bai et al. [25]	—	—	—	—	—/79.3% (Chinese); 80.5% (United States)	68.7% (Chinese); 99% (United States)

Note: all the data were obtained from the literature. The symbol "—" represents data were unavailable. The positive rate, sensitivity, and specificity are expressed as percentage. PT: positive rate; Sen: sensitivity; Spe: specificity.

4. CT Features

It has been reported that pneumonia is the underlying cause of lung injury in patients with COVID-19 [28]. Therefore, the pulmonary lesions in COVID-19 are likely to be similar to those of other types of pneumonia. The majority of patients with COVID show bilateral involvement [10]. In this context, the common findings of CT can highlight the suspected or confirmed cases of COVID-19 infections. Based on the published literature on chest CT findings in relation to COVID-19, the most common features are pure GGOs, appearance of crazy-paving pattern, consolidations, thickening of interlobular septa, reticular pattern, mixed pattern, air bronchogram sign, and bronchiolectasis, among others. Furthermore, the cardinal hallmark of COVID-19 is the bilateral and lower distribution of lesions in the peripheral lung. According to previous reports, chest CT findings vary with time and disease severity [8, 10, 29]. In this review, we have delineated the common and main CT findings of COVID-19 in a pictorial fashion.

4.1. GGO. GGOs were first described by the Fleischner Society. GGOs are defined as blurred areas with slightly increased lung density and the absence of shading of the bronchi and edges of blood vessels, which may be attributed to the partial displacement of air resulting from partial air filling or interstitial thickening [30].

Generally, single or multiple GGOs are observed in patients with COVID-19, either unilaterally or bilaterally, and are distributed peripherally in the subpleural area of the lung [29, 31, 32] (Figure 1(a)). In a study by Shi and coworkers [29], the most common pattern seen in the chest CT of 53 (65%) patients is GGO, and the presence of GGOs is likely to be the earliest CT finding in some patients, which usually appear on 0–5 days after the onset of initial symptoms [8, 33–36]. These results were consistent with those of subsequent studies on pregnant and perinatal women [37], which suggested GGO was the most common and early imaging characteristic, with the occurrence rate of up to 97.6% (81/83)–100% [9, 38, 39]. It is not yet to be understood why GGOs are the early CT manifestations, as the exact pathophysiological mechanism is poorly understood. The early pathological finding is diffuse alveolar damage, as the hyaline membrane between the alveolar walls, alveolar exudation, and edema are not obvious [34, 40]. This finding was supported by another study by Xu and coworkers, in which they performed an autopsy in a patient with COVID-19 [41]. The results demonstrated the presence of slight pulmonary edema and a hyaline membrane between the alveolar walls. Presumably, the above findings may explain the appearance of GGOs in the chest images of patients with COVID-19 (Table 2).

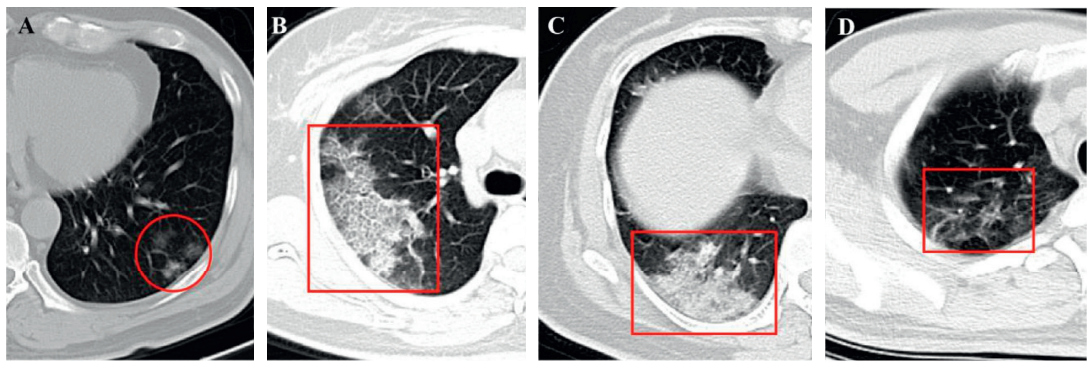

Figure 1: (a) A 46-year-old male COVID-19 patient with no obvious symptoms. CT scan shows three GGOs in the left lower lobe (red cycle). (b) A 46-year-old female COVID-19 patient with fever for 1 day. CT scan demonstrates crazy-paving pattern in the right upper lobe (red rectangle) (5 days after the onset of initial symptoms). (c) The same patient in (b) and the follow-up CT shows the consolidation in the right lower lobe (red rectangle) (8 days after the onset of initial symptoms). (d) A 38-year-old male COVID-19 patient with initial symptoms of dry cough and fatigue for 10+ days. CT scan shows the interlobular septal thickening in the right lower lobe (red rectangle) (7 days after the onset of initial symptoms).

Table 2: The most frequent CT findings acquired from the published literature.

Ref.	*N*	GGO	Crazy-paving pattern	Consolidation	GGO + consolidation	Interlobular septal thickening
Li et al. [38]	83	97.6% (81/83)	36.1% (30)	63.9% (53)	—	62.7% (52)
Guan et al. [42]	47	100% (47/47)	89.4% (42/47)	63.8% (30/47)	—	—
Miao et al. [43]	54*	70.4% (38/54)	29.6% (16/54)	22.2% (12/54)	—	
Zhang et al. [44]	60	97% (58/60)	92% (55/60)	—	—	—
Zhang et al. [45]	34	52.9% (18/34)	23.5% (8/34)	8.8% (3/34)	35.3% (12/34)	—
Gervaise et al. [46]	72	94% (68/72)	38% (27/72)	68% (49/72)	—	—
Dai et al. [47]	219	94.5% (207/219)	—	—	—	93.6% (205/219)
Han et al. [34]	108	60.1% (65/108)	39.8% (43/108)	5.5% (6/108)	40.7% (44/108)	—
Li and Xia [48]	51	35.3% (18/51)	—	5.9% (3/51)	54.9% (28/51)	70.6% (36/51)
Bernheim et al. [10]	121	61.2% (74/121)	4.9% (6/121)			
Zhao et al. [9]	101	86.1% (87/101)	—	43.6% (44/101)	64.4% (65/101)	
Wang et al. [49]	110	27.3% (30/110)	—	27.3% (30/110)	45.4% (50/110)	—
Zhou et al. [33]	62	40.3% (25/62)	—	33.9% (21/62)	—	—
Xiong et al. [50]	42	100% (42/42)	—	81% (34/42)		69% (29/42)
Yoon et al. [51]	9 (40 lesions)	35% (14/40)	10% (4/40)	5% (2/40)	50% (20/40)	—
Cheng et al. [39]	11	100% (11/11)	—	54.5% (6/11)	63.6% (7/11)	
Zhou et al. [52]	100 (272 CT scans)	28.3% (77/272)	—	14% (38/272)	28.3% (77/272)	
Guan et al. [53]	52	96.2% (50/52)	88.5% (46/52)	78.8% (41/52)	—	
Liu et al. [54]	112	35.7% (40/112)	21.4% (24/112)	13.4% (15/112)	50.9% (57/112)	66.1% (74/112)
Hu et al. [55]	46	39.1% (18/46)	—		60.9% (28/46)	2.2% (1/46)
Li et al. [56]	131	15.3% (20/131)	—	3.1% (4/131)	46.6% (61/131)	51.9% (68/131)
Wu et al. [35]	130	53.8% (70/)	76.9% (100)	—	46.2% (60)	—
Zhu et al. [57]	72	50% (36)	—	22.2% (16)	81.9% (59)	—
Wang et al. [58]	13	30.8% (4)	—	7.7% (1)	61.5% (8)	15.4% (2)
Shang et al. [59]	307 (628 CT scans)	—	—	—	—	59.2% (372)
Vancheri et al. [60]	180	21.1% (38)	—	4.4% (8)	68.8% (124)	—
Fan et al. [61]	150	62% (93)	—	4% (6)	34% (51)	—
Luo et al. [62]	70	38.6% (27)	—	2.9% (2)	58.6% (41)	—
Chen et al. [63]	21	95.2% (20)	—	71.4% (15)	—	61.9% (13)
Cecconi et al. [64]	235	68.9% (162)	—	23.8% (56)	—	—
Iwasawa et al. [65]	6	100% (6)	100% (6)	83.3% (5/6)	—	—
Fu et al. [66]	55	32.7% (18)	16.4% (9)	14.5% (8)	52.7% (29)	38.2% (21)
Song et al. [32]	51	76.5% (39)	—	54.9% (28)	58.8% (30)	74.5% (38)
Chung et al. [67]	21	57.1% (12)	19% (4)	0 (0)	28.6% (6)	—
Pan et al. [31]	63	85.7% (54)	—	19% (12)	—	—
Xu et al. [68]	41	73.2% (30)	—	36.6% (15)	61% (25)	80.5% (33)
Wu et al. [69]	80	91.3% (73)	28.8% (23)	62.5% (50)	—	58.8% (47)
Shi et al. [29]	81	65.4% (53)	9.9% (8)	17.3% (14)	13.6% (11)	34.6% (28)
Xu et al. [70]	90	72.2% (65)	12.2% (11)	13.3% (12)	—	36.7% (33)

Table 2: Continued.

Ref.	*N*	GGO	Crazy-paving pattern	Consolidation	GGO + consolidation	Interlobular septal thickening
Liu et al. [71]	73	89% (65)	38.4% (28)	11% (8)	—	—
Zhou et al. [72]	62	61.3% (38)	25.8% (16)	1.6% (1)	35.5% (22)	—
Wang et al. [73]	1012 (917 CT scans)	94.1% (863)	—	5.9% (54)	—	—
Caruso et al. [74]	58	100% (58)	39.7% (23)	72.4% (42)	—	13.8% (8)
Himoto et al. [75]	6	66.7% (4)	0 (0)	0 (0)	33.3% (2)	—
Long et al. [1]	36	30.6% (11)	—	16.7% (6)	52.7% (19)	—
Han et al. [76]	17 (65 CT scans)	69.2% (65)	40% (26)	13.8% (9)	—	53.8% (35)
Ai et al. [4]	1014 (888 CT scans)	46.1% (409/888)	—	50.3% (447/888)	—	0.9% (8/888)
Pan et al. [8]	21 (82 CT scans)	73.2% (60)	23.2% (19)	63.4% (52)	—	—
Yang et al. [77]	149 (2376 segments) #	12.1% (287/2376)		7.2% (170/2376)	26.8% (637/2376)	—
Ding et al. [78]	112 (348 CT scans)	89.9% (313)	54.3% (189)	54.3% (189)	—	—

Pure GGOs are most common in patients with COVID-19 and those in the early stages of infection [59]. However, in an increasing number of cases, GGOs have been found to be accompanied by other signs, including reticular pattern and/or thickening of interlobular septa, appearance of crazy-paving patterns, and consolidations [8, 32, 52]. With the progression of the disease, the appearance of the typical round GGOs decreases, but the appearance of patchy GGOs and consolidations increases. We therefore hypothesize that the appearance of GGOs together with other signs may indicate disease progression and the worsening of lung injury [53].

4.2. Crazy-Paving Patterns. The crazy-paving pattern is another important CT feature, which shows GGOs with superimposed interlobular and intralobular septal thickening, akin to irregular paving stones [30] (Figure 1(b)), and is not as common as GGOs [42–44]. The appearance of crazy-paving patterns is frequently observed in CT findings during disease progression (5–8 days after the illness) or in severe cases of COVID-19 [8, 38, 79]. Based on the previous pathological observations for SARS-CoV, it can be hypothesized that this pattern is caused by acute and severe pulmonary injury with alveolar edema and interstitial inflammation [80]. It has been reported that the percentage of occurrence of crazy-paving patterns varies greatly. The majority of patients with COVID-19 show the appearance of crazy-paving patterns in chest images, and the rate of occurrence can be as high as 92% [44]. However, it has also been reported that this sign may not appear in the chest images of some cases of COVID-19 [47]. Although the rate of occurrence of crazy-paving patterns is relatively lower than that of GGO, it is considered to be a specific sign of COVID-19 [34] (Table 2).

4.3. Consolidations. Pulmonary consolidation refers to the replacement of alveolar air by pathological fluids, cells, or tissues and manifests an increase in the density of the lung parenchyma, resulting in obscuring the margins of vessels and airway walls [30], which usually is observed in the progressive or the peak stage (4–14 days after the onset of the initial symptoms) [8], but it can also be observed in the early stage (0–5 days) [36]. Angiotensin-converting enzyme is a key molecule that is involved in the development of acute lung failure [81]. Similarly, angiotensin-converting enzyme may directly induce pulmonary injury in patients with COVID-19 due to the disequilibrium of the renin-angiotensin system (RAS), which leads to diffuse alveolar damage [82]. Additionally, the appearance of consolidations may correlate with cellular fibromyxoid exudates in the alveoli [41]. These are the likely causes of the appearance of consolidations and account for the rapid changes in clinical manifestations and CT findings. Additionally, the appearance of consolidation is obvious in the progressive stages or in patient cohorts with severe COVID-19 infections [8, 29, 38]. The underlying mechanism of consolidation is in accordance with the pathological changes in the lungs of patients with COVID-19, which demonstrates all components of diffuse alveolar damage, including damage to alveolar epithelial cells, formation of a hyaline membrane, and hyperplasia of type II pneumocytes. In particular, consolidation by fibroblastic proliferation with extracellular matrix and fibrin formation are prominent among patients with COVID-19 [83].

The main CT characteristics of consolidation are multiple, patchy, or segmental regions that are distributed in the subpleural areas or along the bronchovascular bundles [9, 49, 84] (Figure 1(c)). Similar to GGO, consolidation is one of the most common CT findings among patients with COVID-19 [35, 84]. Wong and coworkers reported that consolidation is the most common CT finding (30/64, 47%), followed by GGOs (21/64, 33%), in patients with COVID-19 [84]. Additionally, consolidation can serve as an indicator of disease progression. A recent study by Zhou and coworkers [52] demonstrated that GGOs (41.9%), GGOs with reticular pattern (58.1%), and GGOs with consolidation (43.0%) are common in the early stages (1–7 days) of infection, as observed from 272 CT scans of 100 patients with COVID-19. However, the cardinal CT finding in the advanced stages (8–14 days) is GGOs with consolidation (79.8%), accompanied by repairing CT signs, including the appearance of subpleural line, distortion of the bronchus, and fibrotic strips. Another study demonstrated that pulmonary involvement gradually progressed to consolidation after 5–8 days of the initial

onset of the symptoms [8]. In the progressive stage, GGOs usually evolve to consolidations and coexist with consolidations [8, 10, 52]. Additionally, the extent of consolidations is more likely to be related to the time interval between the initial onset of symptoms and the time of the CT scan and the age of the patient. Older patients with a longer time interval between the onset of symptoms and CT imaging are more likely to show consolidations [32, 52, 78] (Table 2).

4.4. Interlobular Septal Thickening. Interlobular septa are the 10–20 mm long linear or sheet-like structures that form the lobular borders, which are more or less perpendicular to the peripheral pleura [30]. The lobular septum consists of connective tissue, including lymphatic vessels and pulmonary veins. Patients with COVID-19 infection involving the septa may develop septal thickening, and the appearance of septal thickening is visible on chest CT images (Figure 1(d)). In thin-section CT scans, the septal thickening may appear smooth or nodular, which may facilitate the differential diagnosis of COVID-19 from other complications such as pulmonary edema that occurs in many diseases [30]. In some studies, the occurrence of interlobular septal thickening was found to be relatively high in patients with COVID-19, ranging from 0.9% to 93.6%, although it was not as common as GGOs and consolidation [4, 47, 54], and it was more likely to occur in elderly patients [57] (Table 2).

4.5. Air Bronchogram. The appearance of air bronchogram, represented by a pattern of "air-filled bronchi" with low attenuation, was observed on a background of high-density parenchyma without air [30] (Figure 2(a)). This sign is also a common CT finding recorded in a series of cases of COVID-19 [32, 48], which appears frequently in the progressive stage or the peak stage (4–14 days after the onset of the initial symptoms) [33, 53] and sometimes in the early stage [34]. However, the term of "air bronchogram" appears to be inaccurate owing to the low density of the mucus in the bronchi, which is akin to a gelatinous mucus plug rather than air. In fact, the gelatinous mucus in the bronchi may result in slight bronchial dilatation [85]. In patients with COVID-19, the gelatinous mucus plug appears to be of very low density, similar to that of air, against a background of diseased, high-density lung tissue. Ye and coworkers [85] also inferred that coughing in patients with COVID-19 could be attributed to the presence of this gelatinous mucus and damage to the dilated bronchioles (Table 3).

4.6. Bronchiolectasis. Bronchiolectasis is defined as the dilatation of distant bronchioles, which results from potentially reversible airway inflammation, or more frequently, retractile pulmonary fibrosis [30]. On CT images, bronchiolectasis may appear as cylindrical, varicose, or cystic, depending on the affected bronchi, but it can show a tree-in-bud pattern or appear as centrilobular nodules when the dilated bronchioles are accompanied with the thickening of the bronchial wall and mucoid impaction. In the absorption stage of the disease (usually ≥13 days), traction bronchiolectasis can be observed on the CT images, which appear as small, cystic, tubular airspaces, associated with fibrosis [30] (Figure 2(b)). Bronchiolectasis is less common in patients with COVID-19, but Dai and coworkers reported a high occurrence of up to 79% [47]. Generally, bronchiolectasis occurs in the later stages of the disease, such as in the absorptive stage, and is primarily caused by the development of fibrosis [79, 86] (Table 3).

4.7. Pleural Changes. The pleural changes involve pleural thickening and pleural effusion, and the former is more frequent than the latter [29, 87]. In the study by Zhou and coworkers [33], examination of the pleural changes revealed that 30 patients with COVID-19 (48.4%) showed pleural thickening in CT images, whereas only 6 patients (9.7%) had pleural effusion. Similar results were reported in a meta-analysis study with 4121 patients, in which pleural thickening (27.1%) was found to be more prevalent than pleural effusion (5.3%) [87] (Figures 2(c) and 2(d)). Based on the previous literature on Middle East respiratory syndrome coronavirus (MERS-CoV), pleural effusion may serve as a factor for poorer prognosis [38, 88]. In the study by Martino and coworkers [89] on 62 patients with COVID-19, the rate of occurrence of pleural thickening was 72.6%, which was higher than that of pleural effusion (18%). Additionally, the median value of the lung score, which was used to quantify the severity of lung involvement, was significantly higher in patients with pleural thickening than in those without this finding. Pleural effusion may serve as a potential feature for differentiating COVID-19 from other pulmonary infections, such as influenza A (H1N1) virus infections [90] (Table 2).

4.8. Reticular Pattern. The reticular pattern appears as a complex network of linear opacities on CT images, which is caused by interlobular and intralobular septal thickening due to the infiltration of lymphocytes [30, 41] (Figure 3(a)). In a previous study, postmortem CT revealed reticular infiltration of the lungs with severe bilateral, dense consolidation, whereas histomorphological analysis revealed diffuse alveolar damage in 8 patients [91].

Numerous studies have reported that the appearance of a reticular pattern with interlobular septal thickening is one of the most common CT findings in patients with COVID-19 and is second only to GGOs and consolidations [25, 29, 32, 69]. However, the appearance of a reticular pattern differs greatly, with the percentage of 0 to 81.8%, especially in the early stage of the disease (usually 1–7 days) [39, 52, 72]. The prevalence and frequency of reticular patterns can increase in patients with COVID-19 with disease progression [29, 92]. A study by Hu and coworkers demonstrated that the reticular patterns were obvious in 7 of 20 (45%) patients up to 14 days from the initial onset of symptoms [55]. Some studies have reported that, in some cases, reticular patterns do not appear alone, but are frequently accompanied by GGOs and other signs, including vacuolar sign, fibrotic streaks, appearance of a subpleural line, subpleural transparent line, air bronchogram,

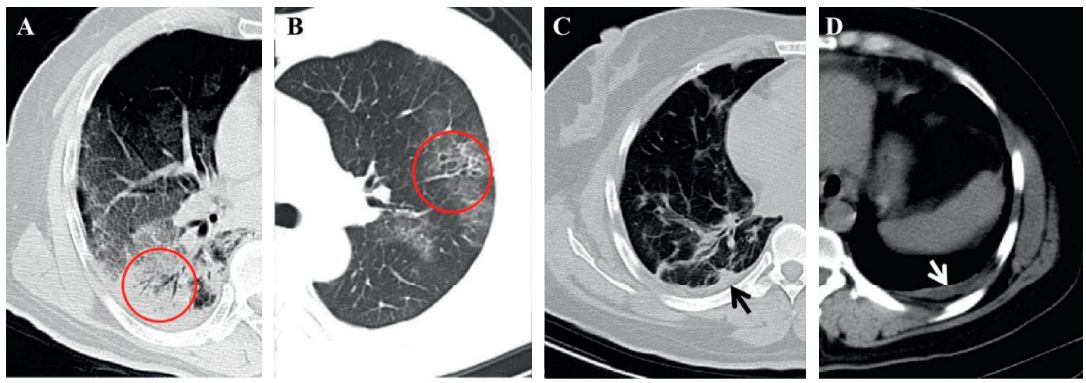

Figure 2: (a) A 60-year-old male COVID-19 patient with initial symptoms of dry cough and fever for 3 days. CT scan shows air bronchogram in the right lower lobe (red circle) (10 days after the onset of initial symptoms). (b) A 46-year-old male COVID-19 patient with fever. CT scan demonstrates bronchiolectasis in the left upper lobe (red circle) (14 days after the onset of initial symptoms), and the bronchial wall thickening is also observed. (c, d) A 40-year-old female confirmed patient with nasal discharge and generalized aches for 11 days. The CT shows the pleural thickening (black arrow) and a small amount of pleural effusion (white arrow) (12 days after the onset of initial symptoms).

Table 3: The less frequent CT findings acquired from the published literature.

Ref.	*N*	Reticular pattern	Air bronchogram	Thickening of the bronchial wall	Bronchiolectasis	Other signs
Li et al. [38]	83	4.8% (4/83)	—	22.9% (19/83)	—	LO: 65.1% (54/83); SWS: 25.3% (21/83)
Guan et al. [42]	47	—	76.6% (36/47)	—	—	Stripe: 57.5% (27/47)
Miao et al. [43]	54*	—	25.9% (14/54)	—	—	PT: 20.4% (11/54)
Zhang et al. [44]	60	—	93% (56/60)	—	—	—
Zhang et al. [45]	34	11.8% (4/34)	41.2% (14/34)	—	—	VE: 50% (17/34)
Gervaise et al. [46]	72	76% (55/72)	—	—	—	PE: 22% (16/72)
Dai et al. [47]	219	61.6% (135/219)	84% (184/219)	34.7% (76/219)	79% (173/219)	PT: 77.6% (170/219)
Han et al. [34]	108	—	48.1% (52/108)	—	—	VT: 79.6% (86/108); HS: 63.9% (69/108)
Li and Xia [48]	51	—	68.6% (35/51)	—	—	VE: 82.4% (42/51)
Bernheim et al. [10]	121	—	—	11.6% (12/121)	0.8% (1/121)	RHS: 1.7% (2/121)
Zhao et al. [9]	101	48.5% (49/101)	—	28.7% (29/101)	52.5% (53/101)	VE: 71.3% (72/101)
Wang et al. [49]	110	—	—	—	—	—
Zhou et al. [33]	62	62.9% (39/62)&	72.6% (45/62)	—	32.2% (20/62)	FS: 56.5% (35/62); VS: 54.8% (34); VE: 45.2% (28/62)
Xiong et al. [50]	42	—	62% (26/42)	—	—	FS: 74% (31/42)
Yoon et al. [51]	9 (40 lesions)	—	27.5% (11/40)	—	—	RHS: 2.5% (1/40)
Cheng et al. [39]	11	81.8% (9/11)	72.7% (8/11)	—	27.3% (3/11)	CN: 27.3% (3/11)
Zhou et al. [52]	100 (272 CT scans)	69.1% (188/272)	57.7% (157/272)	—	—	MD: 45.6% (124/272);VS: 54.8% (149/272)
Guan et al. [53]	52	—	69.2% (36/52)	—	—	IL: 71.2% (37/52)
Liu et al. [54]	112	—	19.6% (22/112)	49.1% (55/112)	—	LO: 64.2% (72/112)

Table 3: Continued.

Ref.	*N*	Reticular pattern	Air bronchogram	Thickening of the bronchial wall	Bronchiolectasis	Other signs
Hu et al. [55]	46	—	69.6% (32/46)	—	—	VE: 89.1% (41/46); HS: 26.1% (12/46)
Li et al. [56]	131	—	57.3% (75/131)	—	—	VE: 64.1% (84/131); fibrosis: 32.8% (43/131)
Wu et al. [35]	130	—	76.9% (100/130)	—	40% (52/130)	PPS: 75.3% (98/130); VT: 76.9% (100/130); HS: 13.8% (18/130)
Zhu et al. [57]	72	61.1% (44/72)	66.7% (48/72)	—	—	VS: 50% (36/72); VE: 45.8% (33/72)
Wang et al. [58]	13	—	46.2% (6/13)	0 (0)	—	—
Shang et al. [59]	307 (628 CT scans)	—	33.6% (211/628)	—	—	VE: 66.2% (416/228)
Vancheri et al. [60]	180	15% (27/180)	—	—	—	PE: 6.6% (12/180)
Fan et al. [61]	150	—	—	—	—	—
Luo et al. [62]	70	—	—	—	—	PT: 17.1 (12/70)
Chen et al. [63]	21	—	57.1% (12/21)	—	—	VE: 66.7% (14/21)
Cecconi et al. [64]	235	—	—	—	—	—
Iwasawa et al. [65]	6	—	—	—	—	LO: 50% (3)
Fu et al. [66]	55	—	52.7% (29/55)	—	—	VT: 81.8% (45/55)
Song et al. [32]	51	21.6% (11/51)	80.3% (41/51)	—	—	PE: 7.8% (4/51)
Chung et al. [67]	21	—	—	—	—	LO: 14.3% (3)
Pan et al. [31]	63	—	—	—	—	FS: 17.5% (11/63)
Xu et al. [68]	41	—	53.7% (22/41)	—	—	TIS: 73.2% (30/41)
Wu et al. [69]	80	—	—	11.3% (9/80)	—	SWS: 25% (20/80); SL: 20% (16/80)
Shi et al. [29]	81	3.7% (3/81)	56.98% (46/81)	—	11.1% (9/81)	PT: 32.1% (26/81)
Xu et al. [70]	90	—	7.8% (7/90)	—	—	LO: 61.1% (55/90); PT: 55.6% (50/90)
Liu et al. [71]	73	—	—	26% (19/73)	—	TLT: 89% (65/73)
Zhou et al. [72]	62	0 (0)	22.6% (14/62)	0 (0)	—	RO: 25.8% (16/62); HS: 11.3% (7/62); SCL 9.7% (6/62)
Wang et al. [73]	1012	—	—	—	—	—
Caruso et al. [74]	58	—	36.2% (21/58)	1.7% (1/58)	41.4% (24/58)	HS: 12.1% (7/68);
Himoto et al. [75]	6	—	—	0 (0)	—	PN: 33.3% (2/6)
Long et al. [1]	36	—	—	—	—	LYM: 2.8% (1/36); PE 5.6% (2/36)
Han et al. [76]	17 (65 CT scans)	0 (0)	41.5% (27/65)	—	3.1% (2/65)	VE: 64.6% (42/65)
Ai et al. [4]	1014 (888 CT scans)	—	—	—	—	NL: 2.7% (24/888)
Pan et al. [8]	21 (82 CT scans)	—	—	—	—	—
Yang et al. [77]	149 (2376 segments)[#]	53% (79/149)	54.4% (81/149)	—	17.4% (26/149)	SLO: 20.8% (31/149); CC: 8.1% (12/149); PE: 6.7% (10/149)
Ding et al. [78]	112 (348 CT scans)	—	36.5% (127/348)	—	25.6% (89/348)	LO: 54% (188/348); PE 17% (59/348)

Note: GGO: ground-glass opacity. The symbol "∗" represents the total number of patients with positive RT-PCR. Symbol "&" represents reticular pattern and GGO. Symbol "#": 149 is the total number of COVID-19 patients. The number in the parentheses represents the total of pulmonary segments in 132 patients with abnormal CT findings ($132 \times 18 = 2376$, 18 pulmonary segments/1 patients). Some percentages are calculated based on the total segments. "—": not available. LO: linear opacities; SWS: spider web sign; PT: pleural thickening; VE: vascular enlargement; VT: vascular thickening; HS: halo sign; RHS: reverse halo sign; FS: fibrous stripes; VS: vacuolar sign; CN: centrilobular nodules; MD: microvascular dilation; IL: irregular line; PPS: parallel pleura sign; VES: vascular enhancement sign; PE: pleural effusion; SL: subpleural line; TIS: thickened intralobular septa; TLT: thickening of lung texture; RO: rounded opacities; SCL: subpleural curvilinear line; PN: pulmonary nodules; LYM: Lymphadenopathy; NL: nodular lesions; SLO: subpleural linear opacity; CC: cystic change.

distortion of the bronchus, and pleural effusion, among others [33, 52, 60] (Table 3).

4.9. Thickening of the Bronchial Wall. The thickening of the bronchial wall is less common and always appears along with bronchiectasis, bronchiolectasis, and respiratory bronchiolitis-interstitial lung disease [30]. Therefore, this finding is frequently observed in critically ill patients or patients in the later stages of the disease, rather than those in the early stages [38]. Based on the literature retrieved till 17 June 2020, the highest rate of occurrence was 49.1% (55/112) [54]. The rates of occurrence reported in other studies were 1.7%–34.7% [9, 10, 38, 47, 69, 71, 74]. On CT images, the thickening of the bronchial wall shows a circular or cystic shape with thickened walls, which resembles a ring and is known as the ring sign [30] (Figure 3(b)) (Table 3).

4.10. Vascular Enlargement. Vascular enlargement refers to the dilatation of blood vessels around or inside the pulmonary lesions, which is always accompanied by GGOs and/or consolidation [9, 48] (Figure 3(c)). Although this sign has been rarely reported, some previous studies have reported that the incidence of this sign can be high in CT images. In a study on 143 patients with COVID-19 infection, initial abnormal chest CT revealed the occurrence of pulmonary vascular dilation in 41 of 46 patients (89.13%) in the early stage (usually 1–5 days after the onset of the symptoms) [55]. Li and Xia reported that vascular enlargement occurred in approximately 82.4% of the patients in their study [48]. Based on the reports of the published literature, vascular enlargement may be caused by alveolar and interstitial pulmonary injury and edema. The novel SARS-CoV-2 virus invades host cells through the cellular angiotensin-converting enzyme II (ACE2) receptor, and the excessive activation of immune cells leads to the production of a large quantity of inflammatory cytokines, including interleukin-6 (IL-6), which results in diffuse injury of pulmonary capillary endothelial cells and alveolar epithelium [28] (Table 3).

4.11. Fibrosis. Some studies have demonstrated that chest CT images of patients with COVID-19 infections show the feature of fibrosis, which is displayed in the shape of stripes, reticulations, or even honeycomb patterns [30, 31] (Figure 3(d)). The appearance of fibrosis may either indicate that the pulmonary lesions have been absorbed, or signify fibrous hyperplasia. However, evidence shows that fibrosis is more likely to develop in patients with severe infections, especially in those with high levels of inflammatory indicators, including C-reactive protein (CRP) and IL-6, and longer periods of hospitalization. During the process of COVID-19 infections, the appearance of interstitial thickening, irregular interface, coarse reticular pattern, and parenchymal band may be considered as predictors of pulmonary fibrosis, especially the appearance of an irregular interface and parenchymal band [92]. As fibrosis deteriorates with disease progression [59], patients with severe infections should be attended to more carefully, as the fibrotic changes are progressive and may result in irreversible interstitial lung disease. This may lead to the decline of pulmonary function, worsening of symptoms, poor quality of life, and early mortality [93] (Table 3). In another study by Lim and coworkers [86], as the COVID-19 improved, the resolution of a lung consolidation and development of a reticular pattern, septal thickening, and bronchiolectasis were the suggestions of fibrosis on the following second week.

At present, the relationship between fibrosis and patient prognosis is controversial. Some studies have reported that fibrosis is a reliable indicator for good prognosis, which suggests the lesions are absorbed significantly and the patient is in a stable condition [31, 35, 94]. However, some researchers support the argument that fibrosis might be an indicator of a poor prognosis because it may result in interstitial lung disease [8, 95, 96].

4.12. Nodules. On CT images, a nodule is defined as a round or irregular opacity which is less than 3 cm in diameter and has well or ill-defined margins [30] (Figure 4(a)). Nodules are of five types, based on the size, location, and density, and are described hereafter. Centrilobular nodules, which are located in the pleural surfaces, fissures, and interlobular septa, show soft tissue or ground-glass attenuation, with sizes ranging from a few millimeters to a centimeter. The second type of nodules is micronodules which have diameters less than 3 mm. Ground-glass nodules manifest as regions of hazy, increased attenuation in the lung, while a solid nodule appears as homogeneous soft tissue attenuation. The fifth type of nodule is the part-solid nodule or semisolid nodule, which consists of both ground-glass and solid soft tissue attenuation components [30]. The appearance of nodules is usually associated with viral pneumonia [97] and could be the initial manifestation of pneumonia caused by COVID-19 [98]. Studies have reported that multifocal solid irregular nodules were observed in 2.7–33.3% of COVID-19 patients [4, 75], while another study reported the presence of nodules with visible halo sign [55] (Table 3).

4.13. Halo Signs and Reversed Halo Signs. The halo sign is a terminology used in CT, which has the features of a nodule or mass surrounded by GGO [30] (Figure 4(b)). The halo sign is less common and not specific for pneumonia resulting from COVID-19, although it has been reported in several studies [34, 48, 99]. The reason underlying the appearance of this sign is unclear and could be related to angioinvasive fungal infections or hypervascular metastases that result in the development of hemorrhage around lesions, viral infections, and organizing pneumonia [30, 100, 101].

On the contrary, the reversed halo sign, which is an atoll sign, is a focal rounded GGO area surrounded by a complete or incomplete circular consolidation (Figure 4(c)). It is an uncommon sign, which was first reported specifically in cryptogenic organizing pneumonia [102], but has been subsequently associated with other diseases [103, 104].

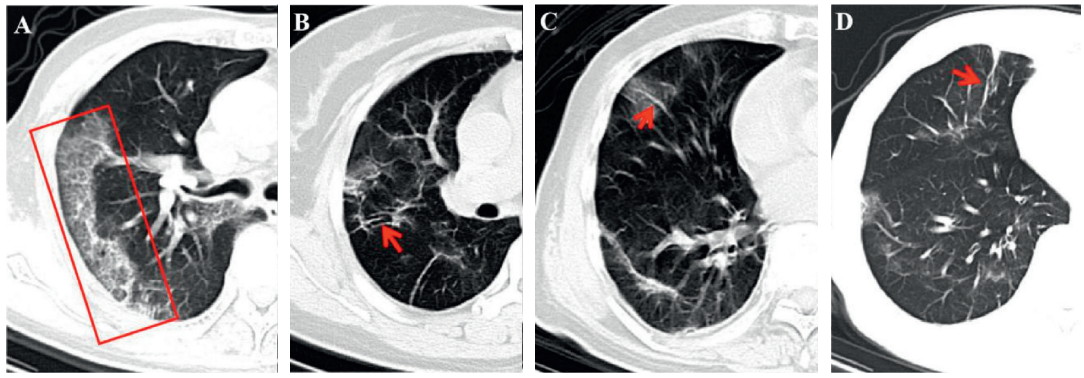

Figure 3: (a) A 79-year-old male COVID-19 patient with prolonged fever for 10 days. The CT displays the reticular pattern in the right upper lobe (red rectangle) (5 days after the onset of initial symptoms). (b) A 40-year-old female confirmed patient with running nose and whole-body pain for 11 days. The bronchial wall thickening is demonstrated on the follow-up CT (20 days after initial symptoms onset) (red arrow). (c) A 79-year-old male COVID-19 patient with prolonged fever for 10 days. The CT displays the vascular enlargement through the lesion in the right middle lobe (red arrow) (4 days after the onset of initial symptoms). (d) The same patient in (c) and the fibrosis is left after treatment for 10 days (red arrow).

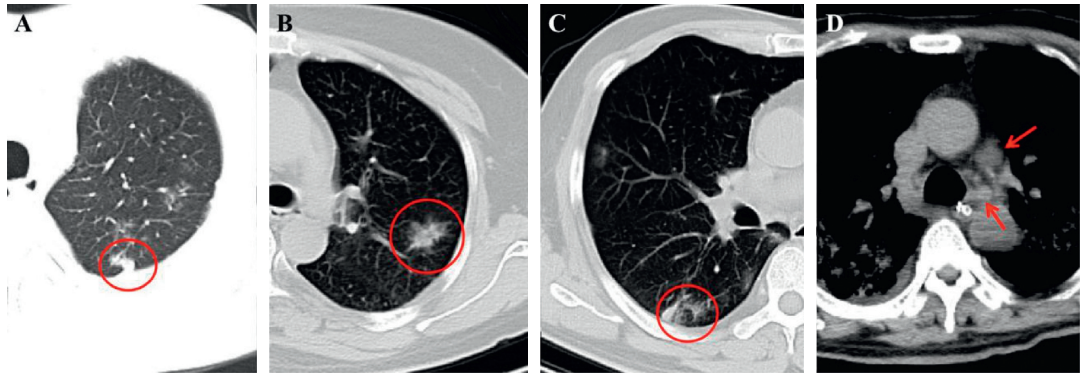

Figure 4: (a) A 46-year-old male COVID-19 patient with fever. CT scan demonstrates a subpleural nodule in the left upper lobe (red circle). (b) A 50-year-old female COVID-19-confirmed patient with dry cough for 4 days. The nontypical halo sign can be seen in the left upper lobe (red circle). (c) The same patient in (a) and the CT displays a nontypical reversed halo sign in the right lower lobe (red circle) in the follow-up CT image. (d) A 60-year-old male COVID-19 patient with initial symptoms of dry cough and fever for 3 days. CT scan shows the enlarged lymph nodes in the mediastinum (red arrows), and this patient is diagnosed coinfection with other bacteria.

Although numerous studies have reported this sign in patients with COVID-19, it is less common than the other signs described herein [35, 55, 74]. Li and Xia [48] reported that the reversed halo sign and pulmonary nodules with a halo sign were observed in 2 (3.9%) and 9 (17.6%) patients with COVID-19, but this sign has not been observed in patients infected with SARS-CoV or MERS-CoV. This sign may be interpreted as disease progression, which induces the formation of consolidations around GGOs or the partial absorption of lesions, leaving a low-attenuation area in the center of the lesion (Table 3).

4.14. Lymphadenopathy. Lymphadenopathy is not common in the COVID-19 patients. The lymphadenopathy is defined when the mediastinal lymph node short-axis diameter is more than 1 cm [30] (Figure 4(d)). This finding was reported in many studies in COVID-19 patients with the percentage of 2.7%–8% [29, 69]. In particular, lymphadenopathy was considered as a likely significant risk factor for COVID-19-patients with severe/critical pneumonia [38, 79]. However, the double or multiple bacterial infections or other viral pneumonia should be considered when lymphadenopathy sign with pleural effusion and small lung nodules are observed [3, 4, 24, 25] (Table 3).

4.15. Other Signs. Besides the abovementioned findings, the other uncommon or rare signs were also reported by some studies, including linear opacities [38, 78], spider web sign [38, 69], vacuolar sign [33, 52, 57], subpleural line [69, 72], and cystic change [77] (Table 3).

4.16. CT Findings in Children and Pregnant Women. Although COVID-19 is more common in adults, it can also occur in neonates, infants, children, and pregnant women

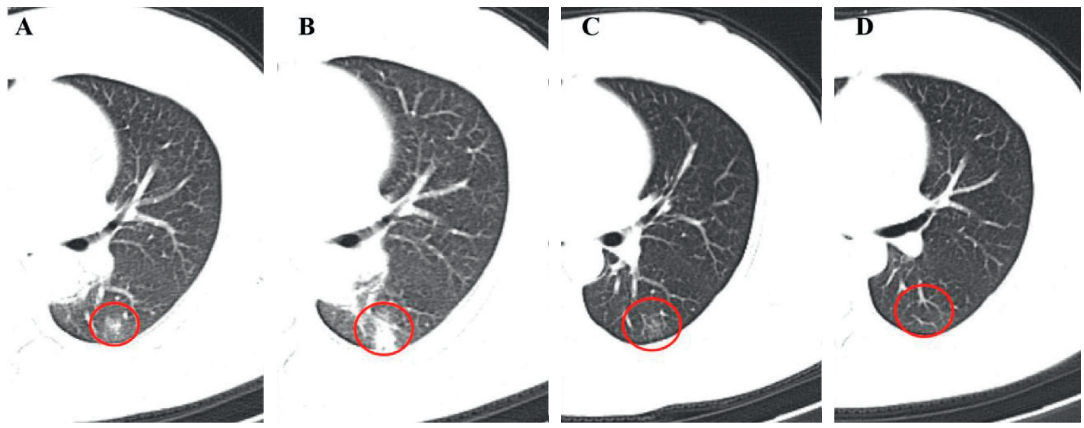

Figure 5: A 46-year-old female COVID-19 patient. On the initial CT (2 days after the initial symptom onset), the patchy GGO was shown in the left lower lung lobe (a) (red circle), but the lesion progressed to large opacities after approximate 5 days, with more lung tissues involvement (b). After regular treatment in hospital, the majority of the lesion was absorbed and dissipated (14 days), with little linear fibrotic lesions left (c). The lesion was absorbed completely on day 22 (d).

[105–107]. In addition, some CT findings may be different from the adults. Therefore, we summarized some common CT findings of confirmed children and pregnant women, based on the published literature except the infants, because the diagnosis of neonates and infants depends on RT-PCR and related clinical data, and CT examinations cannot be performed on them.

Among children, CT findings were usually negative, and they had less extensive disease on abnormal CT scans compared with the adults [106]. The main and common in children findings were GGOs (14%–75%), consolidation (5.2%–70%), and GGO mixed with consolidation lesions (up to 36%) [99, 107–111]. The other signs, including crazy paving pattern, and the halo and reverse halo signs were also observed, which were proved to have a positive correlation between increasing age and increasing severity of findings [106]. However, Xia and coworkers [99] revealed the consolidation with surrounding halo sign was considered to be a typical sign in pediatric patients, which accounted for up to 50% cases.

In pregnant women, the most common CT finding is different. Mixed consolidation and complete consolidation were more common in the laboratory-confirmed and clinically diagnosed pregnant groups [107]. Wu and coworkers [112] found there were 65.2% of patients with patchy GGO in a single lung lobe and 34.8% patients with multiple patchy ground-glass shadows, consolidation, and fibrous stripes, and the similar result was also found in a study by Liu and coworkers [37]; they reported the most common early finding on chest CT was GGO, and with disease progression, crazy paving pattern and consolidations were seen on CT. About the different results, we infer it may be due to the different inclusion criteria, age, and the stage of the patients, which have some impact on the analysis [52, 113].

4.17. The Changes of the CT Findings through the Evolution of COVID-19 Infection. The temporal changes of the radiological features in relation to treatment allocated and the chronological evolution of CT features through the evolution of COVID-19 infection would be of clinical interests, which provide important information for the clinicians.

In a longitudinal study by Wang and coworkers [36], they analyzed the serial CT findings over time in 90 COVID-19 pneumonia patients. The CT scores and number of lobes involved progressed rapidly, peaked during illness days 6–11, and remained at a high level. The predominant pattern of abnormalities after symptom onset was GGO with the percentage from 45% (12–17 days) to 62% (0–5 days), and the consolidation was the second most common finding during illness days 0–5 and 6–11, with the percentage of 23% and 24%, respectively. From illness days of 0–5 to 12–17, the percentage of GGO dropped significantly from 62% to 45%, which was replaced by the significant increase of mixed pattern with the percentage of 1% to 38%, and the mixed pattern became the second most predominant pattern thereafter. The reticular pattern was rarely observed, which was presented on illness days 18–23 and ≥24 with the percentage of 3% and 6%, respectively. These findings reflected the typical pulmonary injury of viral pneumonia, which was characterized by a rapid change as reported in SARS and MERS [114, 115]. As for the temporal change of GGO, pure GGO was also the most common subtype of GGO after symptom onset. GGO with superimposed intralobular lines was the second most common subtype, with the percentage from 8% on illness days 0–5 to 28% on illness days 6–11. Of note, the percentage of GGO demonstrated a trend of "first falling then rising." The percentage significantly dropped down from 65% on illness days 0–5 to 40% on illness days 6–11, with the increased percentages of the other 3 subtypes (GGO with interlobular thickening, GGO with intralobular lines, and irregular lies and interfaces). As the percentage significantly increased up to 71% on illness days 18–23 and thereafter, the other 3 patterns gradually decreased. The changes of these patterns probably reflect the absorption of inflammation and the reexpansion of alveoli, which also indicate the recovery of infection.

In another study with 21 COVID-19 patients by Pan and coworkers [8], GGO, crazy-paving pattern (GGO with superimposed inter- and intralobular septal thickening), and

consolidation were the most common CT features in mild COVID-19. In most cases, the total CT score increased and peaked at 10 days after the onset of symptoms and then gradually decreased, with a total CT score of 6. Four stages were divided based on the quartiles of CT scans and degree of lung involvement from day 0 to day 26 after disease onset: stage 1 (early stage, 0–4 days), stage 2 (progressive stage, 5–8 days), stage 3 (peak stage, 9–13 days), and stage 4 (absorption stage, ≥14 days). The most common CT findings in stage 1 were GGOs with part of crazy-paving pattern and consolidation. Then the GGOs progressed to more pulmonary lobes with more crazy-paving pattern and consolidation in stage 2. In stage 3, consolidation was the main finding, with an significant decrease of GGOs and crazy-paving pattern. In the last stage, the consolidation began to alleviate and was partially absorbed without other signs. Similar results were also found in the study by Ding and coworkers [10, 78] (Figure 5).

Based on the published literature, the most common CT findings in the initial and early stage were GGO and consolidation, including patchy/punctate ground-glass opacities, and most of the GGOs progressed to multiple ground-glass infiltration in the lungs, and the consolidation became more serious in more cases in the progressive, late, or the follow-up stages. The other accompanied features included crazy-paving pattern, interstitial thickening or reticulation, air bronchograms, pleural effusion, and fibrous strips [8, 10, 31, 34, 50, 53, 55].

5. Conclusion

In summary, an early diagnosis and better understanding of COVID-19 infections are crucial for the treatment and management of the disease. This review comprehensively discussed the latest published literature and first-hand interpretation of CT images of pneumonia resulting from COVID-19. The review consolidates the importance of CT imaging in the diagnosis and management of COVID-19, especially in patients showing false-negative results in RT-PCR or having no obvious symptoms. Although the bilateral and peripheral distribution of GGOs and consolidations are considered to be the most common and typical imaging characteristics of patients with COVID-19 infections, the CT features may vary in different patients and at different time points. In this review, we describe the diagnosis, the typical CT features, and some uncommon CT characteristics of patients with COVID-19, for the aid of clinicians and radiologists in understanding the current diagnostic scenario and CT features for reaching a timely and accurate diagnosis. Moreover, chest CT plays an important role in follow-up, as CT features change with disease progression and expectant treatment, of which clinicians should be immediately informed.

Abbreviations

SARS-CoV-2: Severe acute respiratory syndrome coronavirus 2
MERS: Middle East respiratory syndrome.

Conflicts of Interest

The authors declare that they have no conflicts of interest.

Acknowledgments

This manuscript was edited by Editage. This review was supported by grants from the Nature Science Foundation of China (Grant no. 81701756), Sichuan Provincial Department of Education (Grant no. 18ZB0215), City-School Cooperation Project (Grant no. 18SXHZ0389), and China Scholarship Council (Grant no. CSC201908510078).

References

[1] C. Long, H. Xu, Q. Shen et al., "Diagnosis of the coronavirus disease (COVID-19): rRT-PCR or CT?" *European Journal of Radiology*, vol. 126, Article ID 108961, 2020.

[2] J.-L. He, L. Luo, Z.-D. Luo et al., "Diagnostic performance between CT and initial real-time RT-PCR for clinically suspected 2019 coronavirus disease (COVID-19) patients outside Wuhan, China," *Respiratory Medicine*, vol. 168, Article ID 105980, 2020.

[3] Y. Fang, H. Zhang, J. Xie et al., "Sensitivity of chest CT for COVID-19: comparison to RT-PCR," *Radiology*, vol. 296, no. 2, 2020.

[4] T. Ai, Z. Yang, H. Hou et al., "Correlation of chest CT and RT-PCR testing in coronavirus disease 2019 (COVID-19) in China: a report of 1014 cases," *Radiology*, vol. 296, no. 2, pp. E32–E40, 2020.

[5] J. V. Waller, P. Kaur, A. Tucker et al., "Diagnostic tools for coronavirus disease (COVID-19): comparing CT and RT-PCR viral nucleic acid testing," *American Journal of Roentgenology*, vol. 215, no. 4, pp. 834–838, 2020.

[6] Y. Wang, H. Hou, W. Wang, and W. Wang, "Combination of CT and RT-PCR in the screening or diagnosis of COVID-19," *Journal of Global Health*, vol. 10, no. 1, Article ID 010347, 2020.

[7] D. Wang, B. Hu, C. Hu et al., "Clinical characteristics of 138 hospitalized patients with 2019 novel coronavirus-infected pneumonia in Wuhan, China," *JAMA*, vol. 323, no. 11, pp. 1061–1069, 2020.

[8] F. Pan, T. Ye, P. Sun et al., "Time course of lung changes at chest CT during recovery from coronavirus disease 2019 (COVID-19)," *Radiology*, vol. 295, no. 3, pp. 715–721, 2020.

[9] W. Zhao, Z. Zhong, X. Xie, Q. Yu, and J. Liu, "Relation between chest CT findings and clinical conditions of coronavirus disease (COVID-19) pneumonia: a multicenter study," *American Journal of Roentgenology*, vol. 214, no. 5, pp. 1072–1077, 2020.

[10] A. Bernheim, X. Mei, M. Huang et al., "Chest CT findings in coronavirus disease-19 (COVID-19): relationship to duration of infection," *Radiology*, vol. 295, no. 3, Article ID 200463, 2020.

[11] P. B. van Kasteren, B. van der Veer, S. van den Brink et al., "Comparison of seven commercial RT-PCR diagnostic kits for COVID-19," *Journal of Clinical Virology*, vol. 128, Article ID 104412, 2020.

[12] C. C. Yip, C. C. Ho, J. F. Chan et al., "Development of a novel, genome subtraction-derived, SARS-CoV-2-specific COVID-19-nsp2 real-time RT-PCR assay and its evaluation using clinical specimens," *International Journal of Molecular Sciences*, vol. 21, no. 7, 2020.

[13] R. Liu, H. Han, F. Liu et al., "Positive rate of RT-PCR detection of SARS-CoV-2 infection in 4880 cases from one hospital in Wuhan, China, from Jan to Feb 2020," *Clinica Chimica Acta*, vol. 505, pp. 172–175, 2020.

[14] Y. Li, L. Yao, J. Li et al., "Stability issues of RT-PCR testing of SARS-CoV-2 for hospitalized patients clinically diagnosed with COVID-19," *Journal of Medical Virology*, vol. 92, no. 7, pp. 903–908, 2020.

[15] J. Xie, C. Ding, J. Li et al., "Characteristics of patients with coronavirus disease (COVID-19) confirmed using an IgM-IgG antibody test," *Journal of Medical Virology*, 2020.

[16] A. T. Xiao, Y. X. Tong, and S. Zhang, "False-negative of RT-PCR and prolonged nucleic acid conversion in COVID-19: rather than recurrence," *Journal of Medical Virology*, 2020.

[17] J. Watson, P. F. Whiting, and J. E. Brush, "Interpreting a COVID-19 test result," *BMJ*, vol. 369, p. 1808, 2020.

[18] Y. Wang, H. Kang, X. Liu, and Z. Tong, "Combination of RT-qPCR testing and clinical features for diagnosis of COVID-19 facilitates management of SARS-CoV-2 outbreak," *Journal of Medical Virology*, vol. 92, no. 6, pp. 538-539, 2020.

[19] A. Tahamtan and A. Ardebili, "Real-time RT-PCR in COVID-19 detection: issues affecting the results," *Expert Review of Molecular Diagnostics*, vol. 20, no. 5, pp. 453-454, 2020.

[20] W. Wang, Y. Xu, R. Gao et al., "Detection of SARS-CoV-2 in different types of clinical specimens," *JAMA*, vol. 323, no. 18, pp. 1843-1844, 2020.

[21] T. Phan, "Genetic diversity and evolution of SARS-CoV-2," *Infection, Genetics and Evolution*, vol. 81, Article ID 104260, 2020.

[22] Z. Shen, Y. Xiao, L. Kang et al., "Genomic diversity of severe acute respiratory syndrome-coronavirus 2 in patients with coronavirus disease 2019," *Clinical Infectious Diseases: An Official Publication of the Infectious Diseases Society of America*, vol. 71, no. 15, pp. 713–720, 2020.

[23] G. Ye, H. Lin, S. Chen et al., "Environmental contamination of SARS-CoV-2 in healthcare premises," *Journal of Infection*, vol. 81, no. 2, pp. e1–e5, 2020.

[24] J. P. Kanne, B. P. Little, J. H. Chung, B. M. Elicker, and L. H. Ketai, "Essentials for radiologists on COVID-19: an update-radiology scientific expert panel," *Radiology*, vol. 296, no. 2, 2020.

[25] H. X. Bai, B. Hsieh, Z. Xiong et al., "Performance of radiologists in differentiating COVID-19 from viral pneumonia on chest CT," *Radiology*, vol. 296, no. 2, pp. E46–E54, 2020.

[26] R. Mardani, V. A. Ahmadi, F. Zali et al., "Laboratory parameters in detection of COVID-19 patients with positive RT-PCR; a diagnostic accuracy study," *Archives of Academic Emergency Medicine*, vol. 8, no. 1, p. e43, 2020.

[27] W. J. Guan, Z. Y. Ni, Y. Hu et al., "Clinical characteristics of coronavirus disease 2019 in China," *The New England Journal of Medicine*, vol. 382, no. 18, pp. 1708–1720, 2020.

[28] N. Chen, M. Zhou, X. Dong et al., "Epidemiological and clinical characteristics of 99 cases of 2019 novel coronavirus pneumonia in Wuhan, China: a descriptive study," *The Lancet*, vol. 395, no. 10223, pp. 507–513, 2020.

[29] H. Shi, X. Han, N. Jiang et al., "Radiological findings from 81 patients with COVID-19 pneumonia in Wuhan, China: a descriptive study," *The Lancet Infectious Diseases*, vol. 20, no. 4, pp. 425–434, 2020.

[30] D. M. Hansell, A. A. Bankier, H. MacMahon, T. C. McLoud, N. L. Müller, and J. Remy, "Fleischner Society: glossary of terms for thoracic imaging," *Radiology*, vol. 246, no. 3, pp. 697–722, 2008.

[31] Y. Pan, H. Guan, S. Zhou et al., "Initial CT findings and temporal changes in patients with the novel coronavirus pneumonia (2019-nCoV): a study of 63 patients in Wuhan, China," *European Radiology*, vol. 30, no. 6, pp. 3306–3309, 2020.

[32] F. Song, N. Shi, F. Shan et al., "Emerging 2019 novel coronavirus (2019-nCoV) pneumonia," *Radiology*, vol. 295, no. 1, pp. 210–217, 2020.

[33] S. Zhou, Y. Wang, T. Zhu, and L. Xia, "CT features of coronavirus disease 2019 (COVID-19) pneumonia in 62 patients in Wuhan, China," *American Journal of Roentgenology*, vol. 214, no. 6, pp. 1287–1294, 2020.

[34] R. Han, L. Huang, H. Jiang, J. Dong, H. Peng, and D. Zhang, "Early clinical and CT manifestations of coronavirus disease 2019 (COVID-19) pneumonia," *American Journal of Roentgenology*, vol. 215, no. 2, pp. 338–343, 2020.

[35] J. Wu, J. Pan, D. Teng, X. Xu, J. Feng, and Y. C. Chen, "Interpretation of CT signs of 2019 novel coronavirus (COVID-19) pneumonia," *Europeean Radiology*, vol. 30, no. 10, pp. 5455–5462, 2020.

[36] Y. Wang, C. Dong, Y. Hu et al., "Temporal changes of CT findings in 90 patients with COVID-19 pneumonia: a longitudinal study," *Radiology*, vol. 296, no. 2, 2020.

[37] D. Liu, L. Li, X. Wu et al., "Pregnancy and perinatal outcomes of women with coronavirus disease (COVID-19) pneumonia: a preliminary analysis," *American Journal of Roentgenology*, vol. 215, no. 1, pp. 127–132, 2020.

[38] K. Li, J. Wu, F. Wu et al., "The clinical and chest CT features associated with severe and critical COVID-19 pneumonia," *Investigative Radiology*, vol. 55, no. 6, pp. 327–331, 2020.

[39] Z. Cheng, Y. Lu, Q. Cao et al., "Clinical features and chest CT manifestations of coronavirus disease 2019 (COVID-19) in a single-center study in Shanghai, China," *American Journal of Roentgenology*, vol. 215, no. 1, pp. 121–126, 2020.

[40] C. Huang, Y. Wang, X. Li et al., "Clinical features of patients infected with 2019 novel coronavirus in Wuhan, China," *The Lancet*, vol. 395, no. 10223, pp. 497–506, 2020.

[41] Z. Xu, L. Shi, Y. Wang et al., "Pathological findings of COVID-19 associated with acute respiratory distress syndrome," *The Lancet Respiratory Medicine*, vol. 8, no. 4, pp. 420–422, 2020.

[42] C. S. Guan, Z. B. Lv, S. Yan et al., "Imaging features of coronavirus disease 2019 (COVID-19): evaluation on thin-section CT," *Academic Radiology*, vol. 27, no. 5, pp. 609–613, 2020.

[43] C. Miao, M. Jin, L. Miao et al., "Early chest computed tomography to diagnose COVID-19 from suspected patients: a multicenter retrospective study," *The American Journal of Emergency Medicine*, 2020.

[44] N. Zhang, X. Xu, L. Y. Zhou et al., "Clinical characteristics and chest CT imaging features of critically ill COVID-19 patients," *European Radiology*, 2020.

[45] L. Zhang, X. Kong, X. Li et al., "CT imaging features of 34 patients infected with COVID-19," *Clinical Imaging*, vol. 68, pp. 226–231, 2020.

[46] A. Gervaise, C. Bouzad, E. Peroux, and C. Helissey, "Acute pulmonary embolism in non-hospitalized COVID-19 patients referred to CTPA by emergency department," *European Radiology*, vol. 30, no. 11, pp. 6170–6177, 2020.

[47] H. Dai, X. Zhang, J. Xia et al., "High-resolution chest CT features and clinical characteristics of patients infected with COVID-19 in Jiangsu, China," *International Journal of Infectious Diseases*, vol. 95, pp. 106–112, 2020.

[48] Y. Li and L. Xia, "Coronavirus disease 2019 (COVID-19): role of chest CT in diagnosis and management," *American Journal of Roentgenology*, vol. 214, no. 6, pp. 1280–1286, 2020.

[49] K. Wang, S. Kang, R. Tian, X. Zhang, X. Zhang, and Y. Wang, "Imaging manifestations and diagnostic value of chest CT of coronavirus disease 2019 (COVID-19) in the Xiaogan area," *Clinical Radiology*, vol. 75, no. 5, pp. 341–347, 2020.

[50] Y. Xiong, D. Sun, Y. Liu et al., "Clinical and high-resolution CT features of the COVID-19 infection: comparison of the initial and follow-up changes," *Investigative Radiology*, vol. 55, no. 6, pp. 332–339, 2020.

[51] S. H. Yoon, K. H. Lee, J. Y. Kim et al., "Chest radiographic and CT findings of the 2019 novel coronavirus disease (COVID-19): analysis of nine patients treated in Korea," *Korean Journal of Radiology*, vol. 21, no. 4, pp. 494–500, 2020.

[52] S. Zhou, T. Zhu, Y. Wang, and L. Xia, "Imaging features and evolution on CT in 100 COVID-19 pneumonia patients in Wuhan, China," *European Radiology*, vol. 30, no. 10, pp. 5446–5454, 2020.

[53] C. S. Guan, L. G. Wei, R. M. Xie et al., "CT findings of COVID-19 in follow-up: comparison between progression and recovery," *Diagnostic and Interventional Radiology*, vol. 26, pp. 301–307, 2020.

[54] M. Liu, W. Zeng, Y. Wen, Y. Zheng, F. Lv, and K. Xiao, "COVID-19 pneumonia: CT findings of 122 patients and differentiation from influenza pneumonia," *European Radiology*, vol. 30, pp. 5463–5469, 2020.

[55] Q. Hu, H. Guan, Z. Sun et al., "Early CT features and temporal lung changes in COVID-19 pneumonia in Wuhan, China," *European Journal of Radiology*, vol. 128, Article ID 109017, 2020.

[56] X. Li, W. Zeng, X. Li et al., "CT imaging changes of corona virus disease 2019 (COVID-19): a multi-center study in Southwest China," *Journal of Translational Medicine*, vol. 18, no. 1, p. 154, 2020.

[57] T. Zhu, Y. Wang, S. Zhou, N. Zhang, and L. Xia, "A comparative study of chest computed tomography features in young and older adults with corona virus disease (COVID-19)," *Journal of Thoracic Imaging*, vol. 35, no. 4, 2020.

[58] H. Wang, R. Wei, G. Rao, J. Zhu, and B. Song, "Characteristic CT findings distinguishing 2019 novel coronavirus disease (COVID-19) from influenza pneumonia," *European Radiology*, vol. 30, pp. 4910–4917, 2020.

[59] Y. Shang, C. Xu, F. Jiang et al., "Clinical characteristics and changes of chest CT features in 307 patients with common COVID-19 pneumonia infected SARS-CoV-2: a multicenter study in Jiangsu, China," *International Journal of Infectious Diseases*, vol. 96, pp. 157–162, 2020.

[60] S. G. Vancheri, G. Savietto, F. Ballati et al., "Radiographic findings in 240 patients with COVID-19 pneumonia: time-dependence after the onset of symptoms," *European Radiology*, vol. 30, no. 11, pp. 6161–6169, 2020.

[61] N. Fan, W. Fan, Z. Li, M. Shi, and Y. Liang, "Imaging characteristics of initial chest computed tomography and clinical manifestations of patients with COVID-19 pneumonia," *Japanese Journal of Radiology*, vol. 38, no. 6, pp. 533–538, 2020.

[62] N. Luo, H. Zhang, Y. Zhou et al., "Utility of chest CT in diagnosis of COVID-19 pneumonia," *Diagnostic and Interventional Radiology*, vol. 26, no. 5, pp. 437–442, 2020.

[63] D. Chen, X. Jiang, Y. Hong et al., "Can chest CT features distinguish patients with negative from those with positive initial RT-PCR results for coronavirus disease (COVID-19)?" *American Journal of Roentgenology*, pp. 1–5, 2020.

[64] M. Cecconi, D. Piovani, E. Brunetta et al., "Early predictors of clinical deterioration in a cohort of 239 patients hospitalized for covid-19 infection in Lombardy, Italy," *Journal of Clinical Medicine*, vol. 9, no. 5, 2020.

[65] T. Iwasawa, M. Sato, T. Yamaya et al., "Ultra-high-resolution computed tomography can demonstrate alveolar collapse in novel coronavirus (COVID-19) pneumonia," *Japanese Journal of Radiology*, vol. 38, no. 5, pp. 394–398, 2020.

[66] F. Fu, J. Lou, D. Xi et al., "Chest computed tomography findings of coronavirus disease 2019 (COVID-19) pneumonia," *European Radiology*, vol. 30, no. 10, pp. 5489–5498, 2020.

[67] M. Chung, A. Bernheim, X. Mei et al., "CT imaging features of 2019 novel coronavirus (2019-nCoV)," *Radiology*, vol. 295, no. 1, pp. 202–207, 2020.

[68] Y.-H. Xu, J.-H. Dong, W.-M. An et al., "Clinical and computed tomographic imaging features of novel coronavirus pneumonia caused by SARS-CoV-2," *Journal of Infection*, vol. 80, no. 4, pp. 394–400, 2020.

[69] J. Wu, X. Wu, W. Zeng et al., "Chest CT findings in patients with coronavirus disease 2019 and its relationship with clinical features," *Investigative Radiology*, vol. 55, no. 5, pp. 257–261, 2020.

[70] X. Xu, C. Yu, J. Qu et al., "Imaging and clinical features of patients with 2019 novel coronavirus SARS-CoV-2," *European Journal of Nuclear Medicine and Molecular Imaging*, vol. 47, no. 5, pp. 1275–1280, 2020.

[71] K.-C. Liu, P. Xu, W.-F. Lv et al., "CT manifestations of coronavirus disease-2019: a retrospective analysis of 73 cases by disease severity," *European Journal of Radiology*, vol. 126, Article ID 108941, 2020.

[72] Z. Zhou, D. Guo, C. Li et al., "Coronavirus disease 2019: initial chest CT findings," *European Radiology*, vol. 30, no. 8, pp. 4398–4406, 2020.

[73] X. Wang, J. Fang, Y. Zhu et al., "Clinical characteristics of non-critically ill patients with novel coronavirus infection (COVID-19) in a Fangcang hospital," *Clinical Microbiology and Infection*, vol. 26, no. 8, pp. 1063–1068, 2020.

[74] D. Caruso, M. Zerunian, M. Polici et al., "Chest CT features of COVID-19 in Rome, Italy," *Radiology*, vol. 296, no. 2, 2020.

[75] Y. Himoto, A. Sakata, M. Kirita et al., "Diagnostic performance of chest CT to differentiate COVID-19 pneumonia in non-high-epidemic area in Japan," *Japanese Journal of Radiology*, vol. 38, no. 5, pp. 400–406, 2020.

[76] X. Han, Y. Cao, N. Jiang et al., "Novel coronavirus pneumonia (COVID-19) progression course in 17 discharged patients: comparison of clinical and thin-section CT features during recovery," *Clinical Infectious Diseases*, vol. 71, no. 15, pp. 723–731, 2020.

[77] W. Yang, Q. Cao, L. Qin et al., "Clinical characteristics and imaging manifestations of the 2019 novel coronavirus disease (COVID-19): a multi-center study in Wenzhou city, Zhejiang, China," *Journal of Infection*, vol. 80, no. 4, pp. 388–393, 2020.

[78] X. Ding, J. Xu, J. Zhou, and Q. Long, "Chest CT findings of COVID-19 pneumonia by duration of symptoms," *European Journal of Radiology*, vol. 127, Article ID 109009, 2020.

[79] S. Salehi, A. Abedi, S. Balakrishnan, and A. Gholamrezanezhad, "Coronavirus disease 2019 (COVID-19): a systematic review of imaging findings in 919 patients," *American Journal of Roentgenology*, vol. 215, no. 1, 2020.

[80] K. T. Wong, G. E. Antonio, D. S. C. Hui et al., "Thin-section CT of severe acute respiratory syndrome: evaluation of 73 patients exposed to or with the disease," *Radiology*, vol. 228, no. 2, pp. 395–400, 2003.

[81] Y. Imai, K. Kuba, S. Rao et al., "Angiotensin-converting enzyme 2 protects from severe acute lung failure," *Nature*, vol. 436, no. 7047, pp. 112–116, 2005.

[82] D. D'Ardes, A. Boccatonda, I. Rossi et al., "COVID-19 and RAS: unravelling an unclear relationship," *International Journal of Molecular Sciences*, vol. 21, no. 8, 2020.

[83] S. Tian, Y. Xiong, H. Liu et al., "Pathological study of the 2019 novel coronavirus disease (COVID-19) through postmortem core biopsies," *Modern Pathology*, vol. 33, no. 6, pp. 1007–1014, 2020.

[84] H. Wong, H. Lam, A. H. Fong et al., "Frequency and distribution of chest radiographic findings in COVID-19 positive patients," *Radiology*, vol. 296, no. 2, 2019.

[85] Z. Ye, Y. Zhang, Y. Wang, Z. Huang, and B. Song, "Chest CT manifestations of new coronavirus disease 2019 (COVID-19): a pictorial review," *European Radiology*, vol. 30, pp. 4381–4389, 2020.

[86] Z. Y. Lim, H. W. Khoo, T. Hui et al., "Variable computed tomography appearances of COVID-19," *Singapore Medical Journal*, vol. 61, no. 7, pp. 387–391, 2020.

[87] J. Zhu, Z. Zhong, H. Li et al., "CT imaging features of 4121 patients with COVID-19: a meta-analysis," *Journal of Medical Virology*, vol. 92, no. 7, pp. 891–902, 2020.

[88] K. M. Das, E. Y. Lee, M. A. Enani et al., "CT correlation with outcomes in 15 patients with acute Middle East respiratory syndrome coronavirus," *American Journal of Roentgenology*, vol. 204, no. 4, pp. 736–742, 2015.

[89] A. Martino, E. Fiore, E. M. Mazza et al., "CT features of coronavirus disease 2019 (COVID-19) pneumonia: experience of a single center in Southern Italy," *Le Infezioni in Medicina*, vol. 28, no. 1, pp. 104–110, 2020.

[90] Z. Yin, Z. Kang, D. Yang, S. Ding, H. Luo, and E. Xiao, "A comparison of clinical and chest CT findings in patients with influenza A (H1N1) virus infection and coronavirus disease (COVID-19)," *American Journal of Roentgenology*, vol. 215, pp. 1065–1071, 2020.

[91] D. Wichmann, J. P. Sperhake, M. Lütgehetmann et al., "Autopsy findings and venous thromboembolism in patients with COVID-19 : : a prospective cohort study," *Annals of Internal Medicine*, vol. 173, no. 4, pp. 268–277, 2020.

[92] M. Yu, Y. Liu, D. Xu, R. Zhang, L. Lan, and H. Xu, "Prediction of the development of pulmonary fibrosis using serial thin-section CT and clinical features in patients discharged after treatment for COVID-19 pneumonia," *Korean Journal of Radiology*, vol. 21, no. 6, pp. 746–755, 2020.

[93] P. Spagnolo, E. Balestro, S. Aliberti et al., "Pulmonary fibrosis secondary to COVID-19: a call to arms," *Lancet Respiratory Medicine*, vol. 8, no. 8, pp. 750–752, 2020.

[94] N. Cui, X. Zou, and L. Xu, "Preliminary CT findings of coronavirus disease 2019 (COVID-19)," *Clinical Imaging*, vol. 65, pp. 124–132, 2020.

[95] M. Ding, Q. Zhang, Q. Li, T. Wu, and Y.-z. Huang, "Correlation analysis of the severity and clinical prognosis of 32 cases of patients with COVID-19," *Respiratory Medicine*, vol. 167, Article ID 105981, 2020.

[96] J. Wei, H. Yang, P. Lei et al., "Analysis of thin-section CT in patients with coronavirus disease (COVID-19) after hospital discharge," *Journal of X-ray Science and Technology*, vol. 28, no. 3, pp. 383–389, 2020.

[97] T. Franquet, "Imaging of pulmonary viral pneumonia," *Radiology*, vol. 260, no. 1, pp. 18–39, 2011.

[98] T. Xia, J. Li, J. Gao, and X. Xu, "Small solitary ground-glass nodule on CT as an initial manifestation of coronavirus disease 2019 (COVID-19) pneumonia," *Korean Journal of Radiology*, vol. 21, no. 5, pp. 545–549, 2020.

[99] W. Xia, J. Shao, Y. Guo, X. Peng, Z. Li, and D. Hu, "Clinical and CT features in pediatric patients with COVID-19 infection: different points from adults," *Pediatric Pulmonology*, vol. 55, no. 5, pp. 1169–1174, 2020.

[100] J. E. Kuhlman, E. K. Fishman, and S. S. Siegelman, "Invasive pulmonary aspergillosis in acute leukemia: characteristic findings on CT, the CT halo sign, and the role of CT in early diagnosis," *Radiology*, vol. 157, no. 3, pp. 611–614, 1985.

[101] P. S. Pinto, "The CT halo sign," *Radiology*, vol. 230, no. 1, pp. 109-110, 2004.

[102] S. J. Kim, K. S. Lee, Y. H. Ryu et al., "Reversed halo sign on high-resolution CT of cryptogenic organizing pneumonia: diagnostic implications," *American Journal of Roentgenology*, vol. 180, no. 5, pp. 1251–1254, 2003.

[103] X. Zhan, L. Zhang, Z. Wang, M. Jin, M. Liu, and Z. Tong, "Reversed halo sign: presents in different pulmonary diseases," *PLoS One*, vol. 10, no. 6, Article ID e0128153, 2015.

[104] E. Marchiori, G. Zanetti, G. S. P. Meirelles, D. L. Escuissato, A. S. Souza, and B. Hochhegger, "The reversed halo sign on high-resolution CT in infectious and noninfectious pulmonary diseases," *American Journal of Roentgenology*, vol. 197, no. 1, pp. W69–W75, 2011.

[105] W. Liu, J. Wang, W. Li, Z. Zhou, S. Liu, and Z. Rong, "Clinical characteristics of 19 neonates born to mothers with COVID-19," *Frontiers of Medicine*, vol. 14, no. 2, pp. 193–198, 2020.

[106] S. Steinberger, B. Lin, A. Bernheim et al., "CT features of coronavirus disease (COVID-19) in 30 pediatric patients," *American Journal of Roentgenology*, pp. 1–9, 2020.

[107] H. Liu, F. Liu, J. Li, T. Zhang, D. Wang, and W. Lan, "Clinical and CT imaging features of the COVID-19 pneumonia: focus on pregnant women and children," *Journal of Infection*, vol. 80, no. 5, pp. e7–e13, 2020.

[108] L. Su, X. Ma, H. Yu et al., "The different clinical characteristics of corona virus disease cases between children and their families in China—the character of children with COVID-19," *Emerging Microbes & Infections*, vol. 9, no. 1, pp. 707–713, 2020.

[109] B. Li, J. Shen, L. Li, and C. Yu, "Radiographic and clinical features of children with coronavirus disease (COVID-19) pneumonia," *Indian Pediatrics*, vol. 57, no. 5, pp. 423–426, 2020.

[110] Y. Li, H. Wang, F. Wang et al., "Comparison of hospitalized patients with pneumonia caused by COVID-19 and influenza A in children under 5 years," *International Journal of Infectious Diseases*, vol. 98, pp. 80–83, 2020.

[111] L. Lan, D. Xu, C. Xia, S. Wang, M. Yu, and H. Xu, "Early CT findings of coronavirus disease 2019 (COVID-19) in asymptomatic children: a single-center experience," *Korean Journal of Radiology*, vol. 21, no. 7, pp. 919–924, 2020.

[112] X. Wu, R. Sun, J. Chen, Y. Xie, S. Zhang, and X. Wang, "Radiological findings and clinical characteristics of pregnant women with COVID-19 pneumonia," *International Journal of Gynecology & Obstetrics*, vol. 150, no. 1, pp. 58–63, 2020.

[113] Z. Chen, H. Fan, J. Cai et al., "High-resolution computed tomography manifestations of COVID-19 infections in patients of different ages," *European Journal of Radiology*, vol. 126, Article ID 108972, 2020.

[114] G. C. Ooi, P. L. Khong, N. L. Müller et al., "Severe acute respiratory syndrome: temporal lung changes at thin-section CT in 30 patients," *Radiology*, vol. 230, no. 3, pp. 836–844, 2004.

[115] A. M. Ajlan, R. A. Ahyad, L. G. Jamjoom, A. Alharthy, and T. A. Madani, "Middle East respiratory syndrome coronavirus (MERS-CoV) infection: chest CT findings," *American Journal of Roentgenology*, vol. 203, no. 4, pp. 782–787, 2014.